available at www.sciencedirect.com

ScienceDirect

journal homepage: www.elsevier.com/locate/ecolmodel

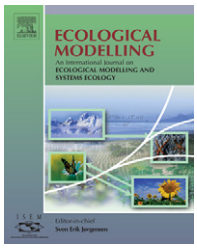

Design and implementation of an integrated GIS-based cellular automata model to characterize forest fire behaviour

S. Yassemi[a], *S. Dragićević*[a,*], *M. Schmidt*[b]

[a] *Spatial Analysis and Modeling Laboratory, Department of Geography, Simon Fraser University, 8888 University Drive, Burnaby, BC V5A 1S6, Canada*

[b] *Department of Geography, Simon Fraser University, 8888 University Drive, Burnaby, BC V5A 1S6, Canada*

ARTICLE INFO

Article history:
Received 20 June 2006
Received in revised form
30 June 2007
Accepted 9 July 2007
Published on line 30 August 2007

Keywords:
Cellular automata
Geographic information system (GIS)
Forest fire behaviour
Spatio-temporal modelling
Simulation methods

ABSTRACT

The integration of geographic information systems (GIS) and environmental modelling has been widely investigated for more than a decade. However, such integration has remained a challenging task due to the temporal changes of environmental processes and the static nature of GIS. This study integrates GIS and cellular automata (CA) techniques to develop a fire behaviour model with a flexible and user-friendly end-user interface. The developed model incorporates topographic, forest fuel and weather variables. The performance of the implemented fire model is evaluated by comparison with fire spread simulations derived from *Prometheus*, the national Canadian fire behaviour modelling tool based on elliptical wave propagation principles. The developed fire behaviour model was tested using spatial data from the 2001 Dogrib Fire near Nordegg Alberta, Canada. Results from the simulations of the CA and wave propagation spread models indicate comparable agreement. This study shows that the GIS-CA model can simulate realistic forest fire scenarios. The developed GIS-based modelling tool enables dynamic animation within the GIS interface. Further, this tool can be adapted to other CA-based spatio-temporal modelling applications.

1. Introduction

Modelling environmental processes and systems enables greater understanding of the natural environment as a whole as well as the relationships and dynamics of its interacting parts. By presenting a simplified or an abstract representation of the world, models can provide insight into the past, define the present or predict the future state of natural phenomena (Smyth, 1998). In this regard, environmental models have been effective in dealing with time and variable interactions, but they traditionally do not incorporate spatial information in the analysis and presentation (Waters, 2002).

Geographical information systems (GIS) have become an indispensable part of environmental modelling technology to manage and analyze increasingly complex and diverse environmental data. GIS have been designed for the collection, retrieval, analysis and display of spatial data (Burrough and McDonnell, 1998), and as such they lack the functionality to represent the temporal dimension or the interactions of continuously changing variables (Dragicevic and Marceau, 2000).

The integration of GIS and spatio-temporal models has been the subject of active research for more than a decade (Clarke et al., 2002). Many approaches of dynamic model integration with GIS have been undertaken. These

* *Corresponding author*. Tel.: +1 778 782 4621; fax: +1 778 782 5841.
E-mail addresses: s_yassemi@alumni.sfu.ca (S. Yassemi), suzanad@sfu.ca (S. Dragićević), schmidtc@sfu.ca (M. Schmidt).
0304-3800/$ – see front matter © 2007 Elsevier B.V. All rights reserved.
doi:10.1016/j.ecolmodel.2007.07.020

strategies can be categorized as: full integration of a model within GIS (embedded coupling); integration under a common interface (tight coupling); linkage through the import/export of data (loose coupling) and incorporation of GIS functionality within the model (Mitasova and Mitas, 2002).

One of the approaches used in enhancing the dynamic modelling capability of raster-based GIS is cellular automata modelling. Cellular automata (CA) were first introduced by Von Neumann (1966) as mathematical representations of complex systems which consist of a grid or lattice of cells where each cell is in one of a number of finite states. The state of a cell depends on a set of rules and the state of the neighbouring cells. Cells change state as a result of deterministic, probabilistic or stochastic transition rules. The time component progresses in discrete steps and the cells update their state synchronously after the transition rules are applied (White and Engelen, 1997; Batty and Xie, 1994). Cellular automata have many characteristics that make them attractive in spatio-temporal modelling. Utilizing simple local rules, they have the potential to model complex phenomena. Moreover, they are inherently spatial and their structure is compatible with geospatial data sets available from various digital sources (White and Engelen, 2000).

CA models have been used to understand a variety of spatial phenomena including plant competition (Grist, 1999; Matsinos and Troumbis, 2002), epidemic propagation and vaccination (Sirakoulis et al., 2000; Morley and Chang, 2004), habitat fragmentation (Darwen and Green, 1996; Balzter et al., 1998), pedestrian traffic flow in fire evacuation (Yang et al., 2002), plant invasion and dispersal (Cannas et al., 2003), spatial dynamics of urban and regional systems (Clarke and Gaydos, 1998; Wu and Webster, 2000), forest insect propagation (Bone et al., 2006), and forest fire propagation (Berjak and Hearne, 2002; Ito, 2005).

In the case of fire events, there are both positive and negative consequences. On the one hand, fire plays an integral role in maintaining the health and diversity of many forest ecosystems (Johnson and Miyanishi, 2001). On the other hand, fire can have negative socio-economic consequences and can adversely impact public health and safety, property and natural resources. As such, there is a constant demand for more effective fire management policies due to the human risks and the rising concern about global climate change. Consequently, a variety of forest fire models and decision support systems are in existence and in continuous development to aid in more effective management (Pastor et al., 2003; Andrews and Queen, 2001). Ecosystem differences and the influence of changing environmental factors are challenges that make many fire models context dependent (Jordan et al., 2005).

The objectives of this study are to: (1) Develop an integrated GIS-based cellular automata fire behaviour model with a flexible and user-friendly modelling environment; and (2) Evaluate the performance of the GIS-CA model by comparison with the fire spread simulations from *Prometheus*, a national Canadian fire modelling tool.

2. Fire behaviour modelling and cellular automata

Mathematical fire behaviour models consist of a set of equations whose solution gives numerical values for one or more variables such as the rate of spread, flame height, ignition risk or fuel consumption that change through time or space. Based on the nature of the equations, these models can be classified as physical (theoretical), empirical (statistical) and semi-empirical (Pastor et al., 2003). Further, based on the variables studied, mathematical models can be divided into fire spread models and fire front properties models.

Fire simulation techniques can be divided into two general categories, those based on regular grid systems and those based on continuous planes (Richards, 1995; Pastor et al., 2003). Bond percolation and cellular automata (regular grid or cellular) and elliptical wave propagation (continuous plane) are among the most widely used techniques for wildland fire simulations. The two techniques differ in how they represent the landscape and the criterion used to simulate fire growth (Albright and Meisner, 1999; Pastor et al., 2003).

With the increase in popularity of computerized modelling, the use of cellular models to simulate fire growth as discrete processes on a regularly spaced landscape grid has been a common approach (Finney, 2004). A number of studies have been reported in the literature dealing with cellular models. Among the first is the study by Kourtz and O'Regan (1971) and Kourtz et al. (1977) using the bond percolation process. Other studies include the transfer of fractional burned area (Karafyllidis and Thanailakis, 1997; Richards, 1988), fractal algorithms (Clarke et al., 1994), and stochastic percolation techniques (Beer and Enting, 1990; Hargrove et al., 2000). Berjak and Hearne (2002) improved on Karafyllidis and Thanailakis's (1997) model by incorporating the Rothermel's (1972) semi-empirical forest fire spread model. De Vasconcelos et al. (2002) based their model on Rothermel's model (1972, 1983) and some extensions of the BEHAVE program (Andrews, 1986) using the object-oriented discrete event specification (DEVS) formalism (Ziegler, 1990).

In the vector or wave propagation models, the fire front is propagated at specified time intervals as a continuously expanding fire polygon (Finney, 2004). This simulation criterion is based on the Huygens wave propagation principle (Anderson et al., 1982). These models assume an ellipsoidal shape for fire growth. In fact, the simple ellipse is the most common model for fire shape under uniform conditions considering forest fuels, weather and topography (Van Wagner, 1969).

According to French (1992) and Finney (2004), under more heterogeneous environmental conditions (e.g. temporal changes in fuel moisture, wind speed and direction, varying topography) cellular models are generally less successful than wave propagation models in reproducing the expected spatial patterns of fire growth. In fact, some present operational fire modelling tools such as FARSITE (U.S.) (Finney, 2004), Prometheus (Canada) (Prometheus, 2004) and SiroFire (Australia) (Coleman and Sullivan, 1996) are based on the elliptical wave model.

In the Prometheus model, the inputs include topographic data such as slope, aspect and elevation, fuel types of the Canadian Fire Behaviour Prediction (FBP) System (Forestry Canada Fire Danger Group, 1992), and the weather stream. Fire behaviour outputs are calculated using the Canadian Fire Weather Index (FWI) (Van Wagner, 1987) and the FBP Systems which constitute the two primary subsystems of the Canadian Forest Fire Danger Rating System (CFFDRS).

The FBP System is an empirical model. By integrating the major factors influencing forest fire spread, it provides quantitative estimates of certain fire behaviour characteristics for 16 major fuel types in Canada based on topography, daily and hourly weather data and certain components of the FWI System as inputs. Primary outputs of the system include rate of spread and direction, fuel consumption, head fire intensity and fire type (e.g. surface, crown) (Forestry Canada Fire Danger Group, 1992; Lee et al., 2002).

This study focuses on developing a deterministic short-range CA-based fire behaviour model with simple and intuitive transition rules. Modeling of fire spread under heterogeneous conditions is specifically addressed by incorporation of fire characteristics calculated by the empirical FBP System. The study improves on previous cellular automata models by utilizing unique and specific deterministic transition rules that enable detailed accounting of fire spread within and between cells as well as synchronization of fire spread with wind and slope directions in a realistic manner. Further, a GIS-based modelling tool with an end-user interface is created to provide a flexible environment for modelling and facilitating the visualization of simulation results. A direct comparison of the cellular and wave approaches of fire spread modelling is provided, as well a critical analysis of the results and their importance in regards to other CA modeling techniques is presented.

3. Methodology

The state of each cell in the CA model is a function of the states of the neighbourhood cells. In this study, a Moore neighbourhood consisting of the eight adjacent cells is considered (Fig. 1(a)). The state of each cell at time t is defined by the proportion of the cell burning (ratio of the burning area to the total cell area). Hence, the state of a cell ranges from 0 (unburned) to 1 (completely burned) along a continuous scale.

The CA transition rules are based on the assumption that fire can spread from a neighbouring cell to the central (i, j) cell only when the neighbour cell is completely burning (i.e. has a state of 1) as shown in Fig. 1(b) for the $(i, j-1)$ neighbour. Once the (i, j) cell is ignited, the fire travels through the cell according to the cell's rate of spread vector that consists of the *speed of fire* (ROS) and its *direction of travel* (RAZ) obtained from the FBP System.

The FBP System is used as the basis of the cellular automata model to provide access to the equilibrium fire spread rate and direction in each cell by accounting for the fuel type, topographic and weather factors. Given the empirical nature of the FBP model and its validation for the major fuel types in Canada, the fire spread rate and direction derived from this

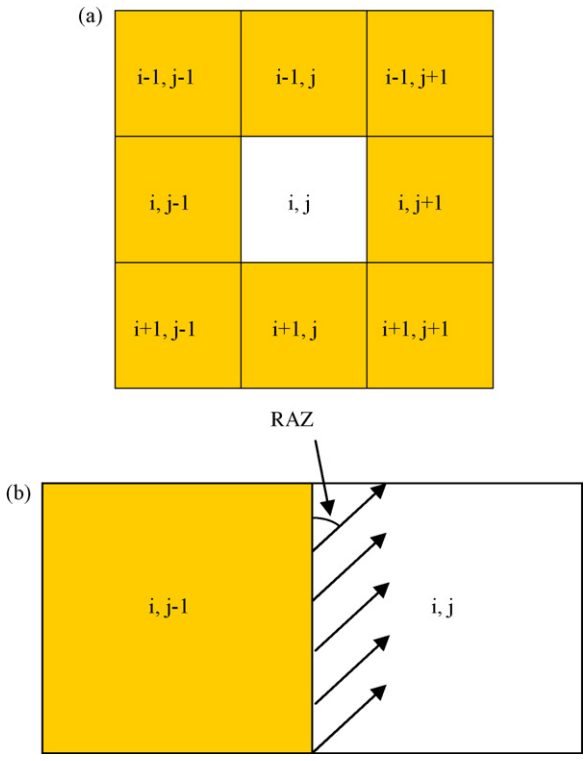

Fig. 1 – (a) CA Moore neighbourhood; (b) fire spreading from west neighbour to (i, j) cell, arrows indicate the fire spread vector.

model are considered valid within each cell. The CA transition rules therefore model the propagation of fire between cells.

The FBP System uses 14 primary inputs classified into five general categories, namely fuels, weather, topography, foliar moisture content, and type and duration of prediction. Three steps are involved in predicting the equilibrium head fire rate of spread (Forestry Canada Fire Danger Group, 1992; Hirsch, 1996): (1) a basic rate of spread is calculated based on empirical data for each fuel type; (2) the interactive effect of both slope (azimuth and steepness) and wind (direction and speed) on the rate and direction of fire spread are calculated; 3) the above rate of spread is modified to account for the amount of fuel that is available for combustion in the entire fuel complex.

The state of the (i, j) cell at each time step Δt is calculated using trigonometry. The magnitude of the appropriate component of the velocity vector is calculated based on RAZ and ROS. Multiplication of the calculated speed by the time interval results in the distance of travel of fire inside the cell in the desired direction and consequently the area burned at the end of the time interval.

Cases involving fire traveling east (west neighbour burning) and northeast (southwest neighbour burning) are discussed below in more detail. The spread of fire from the remaining six neighbours namely northwest, north, northeast, east, south and southeast to the (i, j) cell follows the same logic as the above two cases. Each direction has its own unique range of angles (inside (i, j) cell) used for the calculations of the speed component and distance traveled at each time step. Table 1 summarizes the range of angles permitting fire to

Table 1 – Range of fire direction angles permitting fire spread inside (i, j) cell based on location of burning neighbour

Fire spread from neighbour	Range of angles permitted for fire spread inside (i, j) cell
Northwest	$90^\circ < RAZ < 180^\circ$
North	$90^\circ < RAZ < 270^\circ$
Northeast	$180^\circ < RAZ < 270^\circ$
West	$0^\circ < RAZ < 180^\circ$
East	$180^\circ < RAZ < 360^\circ$
Southwest	$0^\circ < RAZ < 90^\circ$
South	$270^\circ < RAZ < 90^\circ$
Southeast	$270^\circ < RAZ < 360^\circ$

spread inside the (i, j) cell based on the location of the burning neighbour.

3.1. *Fire spreading east from the west neighbour*

Fig. 2(a) and (b) depicts the case of fire spread to the (i, j) cell from an adjacent westerly neighbour. Fire travels in the (i, j) cell (i.e. has a positive easterly component) only if the direction of travel (RAZ) is greater than 0° (north) and less than 180° in this cell. For case (a) where $0 < RAZ \leq 90^\circ$, the east component of velocity vector, ROS_East (m/min), which represents the *speed of fire traveling east* is given by:

$$ROS\_East = ROS * \sin(RAZ) \quad (1)$$

and in case (b) where $90^\circ \leq RAZ < 180^\circ$, speed is derived by:

$$ROS\_East = ROS * \sin(180 - RAZ) \quad (2)$$

The distance of travel (due east) after one time step is calculated by multiplying the horizontal speed by the elapsed time:

$$\Delta x_t = ROS\_East * \Delta t \quad (3)$$

where Δx_t is in meters and Δt is in seconds. After each time step, the distances moving east are summed until the fire reaches the other side and covers the whole cell. The area burned at time *t* is calculated by multiplying the distance traveled east by the cell size.

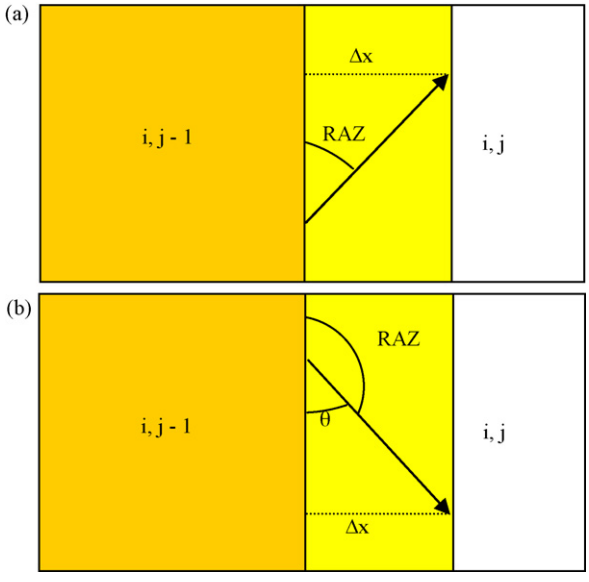

Fig. 2 – Fire spreading east for (a) $0 < RAZ \leq 90^\circ$; (b) $90^\circ \leq RAZ < 180^\circ$.

3.2. *Fire spreading northeast from the southwest neighbour*

Fig. 3 indicates the case of fire spread to the (i, j) cell from its diagonal southwest neighbour. Fire travels in the (i, j) cell (i.e. has positive easterly and northerly components) only if the direction of travel is greater than 0° and less than 90° in this cell. *Speed* (m/min) *of fire traveling east* is given by:

$$ROS\_East = ROS * \sin(RAZ) \quad (5)$$

and *distance* (m) traveled east after one *time interval* (second) is:

$$\Delta x_t = ROS\_East * \Delta t \quad (6)$$

Speed of fire traveling north is calculated by:

$$ROS\_North = ROS * \cos(RAZ) \quad (7)$$

while *distance* traveling north after one *time interval* is given by:

$$\Delta y_t = ROS\_North * \Delta t \quad (8)$$

After each iteration, the distances moving east and north are individually summed until the fire covers the entire cell. The total surface area of the cell burned at time *t* is calculated by multiplying the horizontal by vertical distance of fire travel.

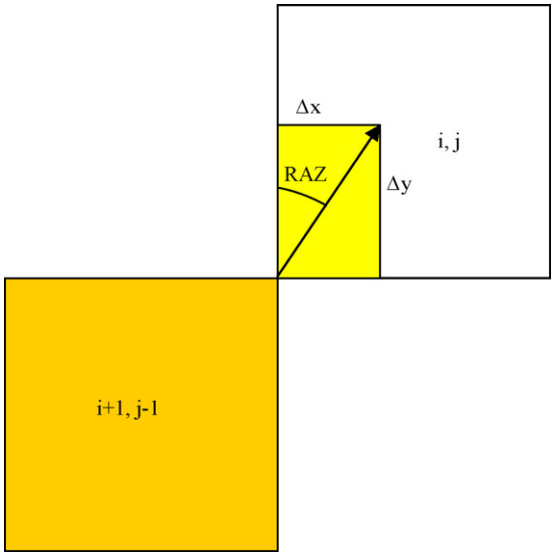

Fig. 3 – Fire spreading northeast for $0 < RAZ < 90^\circ$.

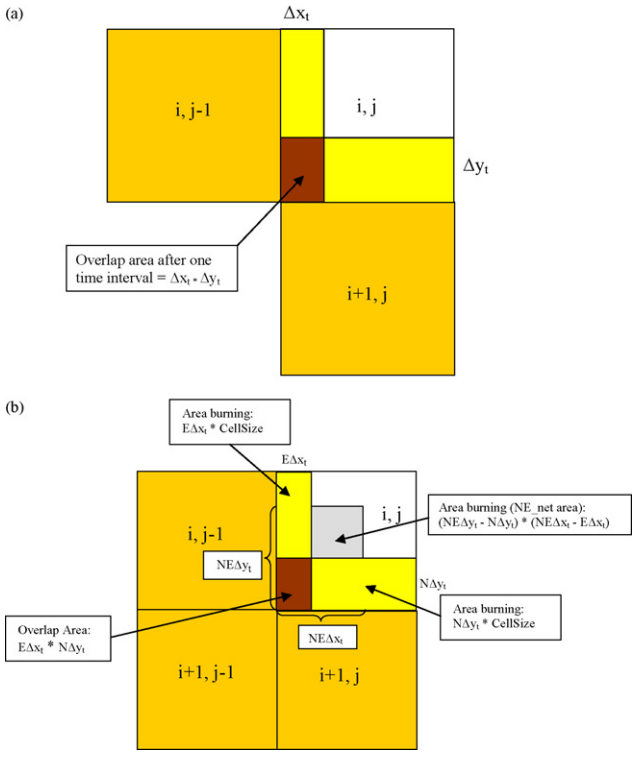

Fig. 4 – Overlap of burning areas from (a) east and north moving fires (b) east, north and northeast moving fires.

3.3. *Accounting for overlaps of the burning areas*

Once the fire spreads to the (*i*, *j*) cell from two or more adjacent neighbours, there will be an overlap of the burning areas. When calculating the state of the cell, summing the burned areas contributed from fire entering the cell from different sides would result in an overestimation of the area burned. This overestimation would affect the validity of the model by simulating a faster spread of fire and hence overestimation of the total area burned. These overlaps are subtracted from the total area burned. Fig. 4(a) gives an example of the overlap for fire moving from south and west throughout the cell.

Adding the contribution of fire from a diagonal neighbour to the above situation would result in a more complex overlapping problem as depicted by Fig. 4(b). If the horizontal (i.e. NE_Δx_t) and vertical component (NE_Δy_t) of the fire traveling northeast (contribution from southwest neighbour) are larger than the horizontal component of the east moving (*E*_Δx_t) and vertical component of the north moving (*N*_Δy_t) fire, then a *net burning area* (NBA) (i.e. NE_net area in Fig. 4(b)) will need to be accounted for and added to the areas contributed from west and south directions. Consequently the NE_net (m^2) within the (*i*, *j*) cell in the case of fire spread from west, southwest and south is:

$$\text{NE\_net} = \text{CellSize} * (E\Delta x_t + N\Delta y_t) + ((\text{NE}\Delta y_t - N\Delta y_t) * (\text{NE}\Delta x_t - E\Delta x_t)) - (E\Delta x_t * N\Delta y_t) \quad (9)$$

The overlap of the diagonal NE moving fire with the north and east moving fire was also calculated. Subtraction of the overlap did not have a measurable effect on the test simulations; therefore it was not incorporated in order to reduce the computational complexity.

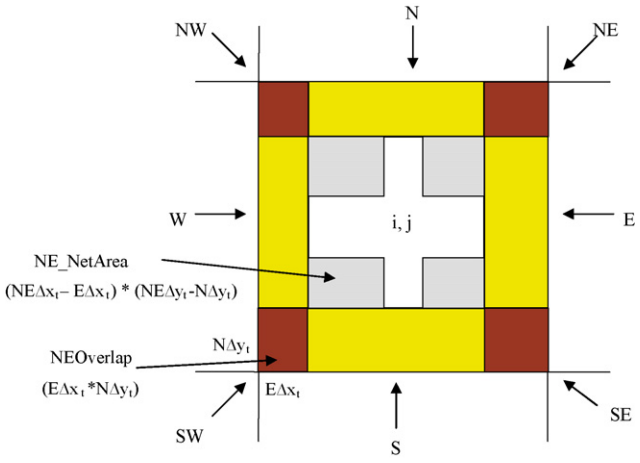

Fig. 5 – Calculation of the net burning area accounting for all overlaps.

It should be noted that once a cell ignites from different sides, the fire will spread in a complex pattern and naturally its behaviour and spread cannot be simply represented by addition and subtraction of rectangular burned areas. This method is used here to account for the over and under-estimations in the burned area within a cell resulting from addition of fire spread contributions from different neighbours.

Following the same logic presented above, a universal equation can be applied to calculate the net burning area within the cell by accounting for overlaps and burning areas contributed from all sides. If a neighbour is not burning, its contribution to the (*i*, *j*) cell will be zero. Fig. 5 shows the derivation of the *net burning area* (NBA) (m^2) for (*i*, *j*) cell which is calculated by:

$$\begin{aligned}\text{NBA}(i,j) = {} & \text{CellSize} * (E\Delta x_t + W\Delta x_t + N\Delta y_t + S\Delta y_t) \\ & + (\text{SE\_NetArea} + \text{SW\_NetArea} + \text{NW\_NetArea} \\ & + \text{NE\_NetArea}) - \text{SEOverlap} - \text{SWOverlap} \\ & - \text{NWOverlap} - \text{NEOverlap}\end{aligned} \quad (10)$$

3.4. *Angle limitation inside neighbouring cells*

The transition rules set no limitation on the direction of fire travel in the burning neighbouring cell, and assume spread of fire if the direction of fire travel in the (*i*, *j*) cell is within the determined ranges. This condition was found to overestimate the spread of fire to a large extent and result in fire spread not properly following the net wind direction. In order to ameliorate this condition, a limiting fire direction range was placed for the burning neighbouring cell as a pre-condition for fire spread into the (*i*, *j*) cell. Fig. 6 shows the conditions placed on fire direction on the west and southwest neighbours respectively. Table 2 lists the range of limiting angles for all neighbours for head fire spread (as well as back fire spread discussed below) for two categories of net wind speeds (WSV).

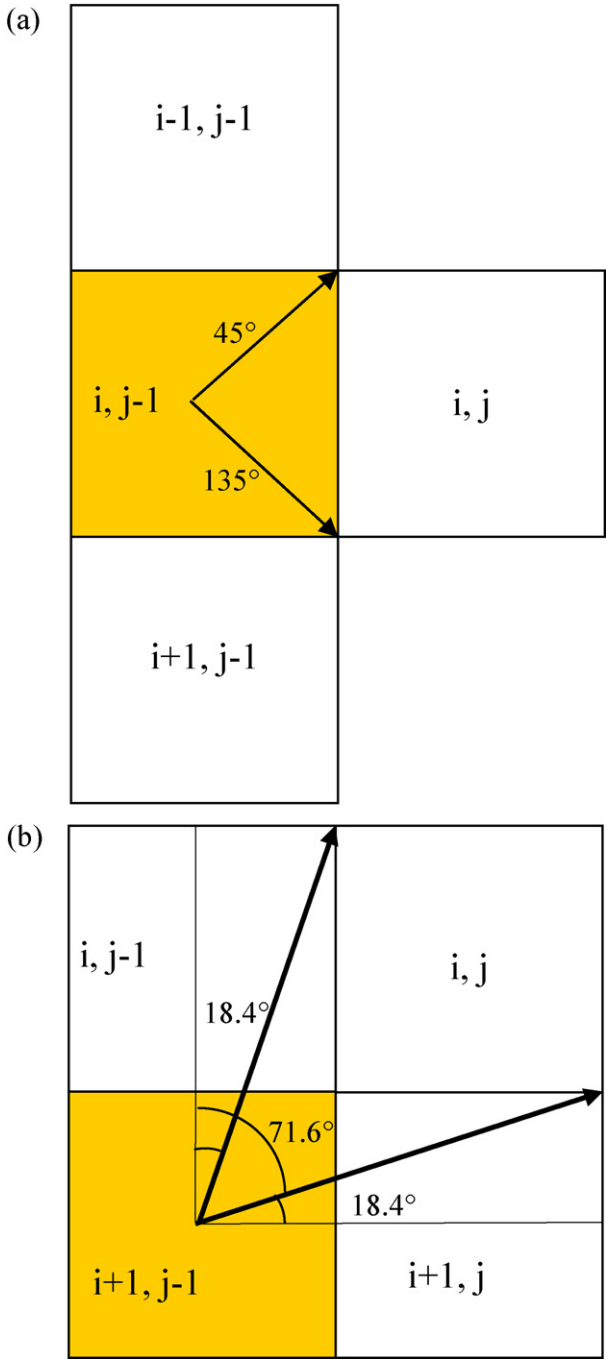

Fig. 6 – Fire direction limits in burning neighbour allowing fire spread to (i, j) cell: (a) 45° < RAZ < 135° in west neighbour; (b) 18° < RAZ < 71° in southwest neighbour.

For example given a fire direction of 40° in a cell, the fire will spread to its north and northeast cells only when net wind speeds are above 20 km/h.

3.5. *Low net wind conditions (gentle terrain and gentle wind)*

The above calculations assume fire spread from a cell to its neighbour based only on the head fire spread. This assumption is valid when the *net wind speed* (WSV) (obtained from the FBP System by converting slope to an "equivalent wind speed" and combining with observed wind speed to determine the net effective wind vector) is relatively high (high wind and/or steep slopes) in which case most of the spread can be attributed to the head fire spread. For this scenario in the elliptical model the fire would have a more elongated shape. However, in low net wind conditions (low angle terrain and gentle wind speed) the back and flank rates assume more importance in the elliptical fire model and the length to breadth ratio of the elliptical fire decreases which in turn leads to a more rounded shape. When WSV is zero, *back spread rate* (BROS) is equal to the *head fire spread rate* (ROS). In homogeneous conditions (flat ground and single fuel type) a zero wind speed would result in a circular fire shape. As the net wind speed increases BROS decays to a near constant, where back fire spread will be self-extinguishing in very high WSV conditions. A back fire spread model was developed in the FBP System using a modified set of equations for ISI (*initial spread index* derived in FWI System) and ROS (Forestry Canada Fire Danger Group, 1992).

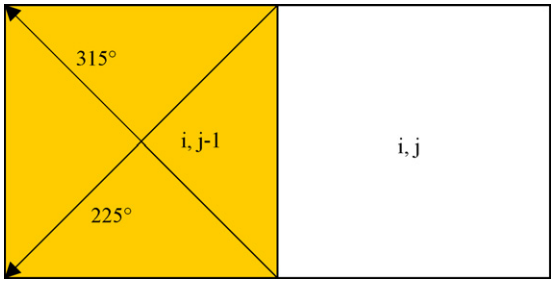

Fig. 7 – Back fire spread to (i, j) cell for WSV ≥ 20 km/h when RAZ in west neighbour is 225° < RAZ < 315°.

In order to account for some of the above changes in fire shape with changing WSV conditions, back fire spread was incorporated in the CA model. However, elliptical flank spread was not accounted for. The calculations for back fire spread are identical to the head fire spread with the difference that BROS (calculated in FBP System) is used as the fire spread rate inside (i, j) cell and the limiting angle range in the burning neighbour is taken to be the reverse mirror of the angle range used for head fire spread. Fig. 7 shows the case of the west neighbour burning and the back fire spread into the (i, j) cell when WSV is greater than 20 km/h. In this case, if the direction of fire in the west neighbour is between 225° and 315° then there will be a back fire spread inside (i, j) cell. Limiting angle ranges for back fire spread for all neighbours are listed in Table 2.

In order to account for conditions of low angle terrain and gentle wind speed (low WSV), the limiting angle ranges in the burning neighbours are relaxed so that fire can spread with more ease to the (i, j) cell and form a more rounded shape. Table 2 also lists the limiting angle ranges for head fire and back fire spread for each neighbour when WSV is greater than 10 km/h and less than 20 km/h. There are no fire direction limits set on neighbours when WSV values are less than 10 km/h. The WSV and angle limitation ranges are set subjectively in order to take into account the above observations.

Table 2 – Range of fire direction angles inside neighbouring cells permitting fire to spread to the (i, j) cell

Neighbour	High net wind speeds (WSV ≥ 20)		Low net wind speeds (10 ≤ WSV ≤ 20)	
	Head fire spread	Back fire spread	Head fire spread	Back fire spread
Northwest	108° < RAZ < 161°	288° < RAZ < 341°	90° < RAZ < 180°	270° < RAZ < 360°
North	135° < RAZ < 225°	315° < RAZ < 45°	90° < RAZ < 270°	270° < RAZ < 90°
Northeast	198° < RAZ < 251°	18° < RAZ < 71°	180° < RAZ < 270°	0° < RAZ < 90°
West	45° < RAZ < 135°	225° < RAZ < 315°	0° < RAZ < 180°	180° < RAZ < 360°
East	225° < RAZ < 315°	45° < RAZ < 135°	180° < RAZ < 360°	0° < RAZ < 180°
Southwest	18° < RAZ < 71°	198° < RAZ < 251°	0° < RAZ < 90°	180° < RAZ < 270°
South	315° < RAZ < 45°	135° < RAZ < 225°	270° < RAZ < 90°	90° < RAZ < 270°
Southeast	288° < RAZ < 341°	108° < RAZ < 161°	270° < RAZ < 360°	90° < RAZ < 180°

4. Development of the integrated GIS-CA modelling tool

The integrated environment was developed using the Idrisi Kilimanjaro GIS software (Clark Labs, 2004) and the Visual Basic programming language. Idrisi is fully component object model (COM) compliant and so by using its application programming interface (API) it is possible to use any COM-compliant programming language to create custom applications as well as develop and integrate new modules within Idrisi (Clark Labs, 2004).

The base logic of the incorporation of CA modelling in the GIS software is the ASCII/raster file conversion and the input/output of files by the GIS and programming environment in a seamless manner. A raster data layer is composed of a matrix of cells with a numeric value assigned to each cell. The raster image is converted to an ASCII grid text file (automated by calling Idrisi's conversion function) which in turn is read and stored in a two-dimensional array in the programming environment (also automated programmatically). The parameters of the ASCII file (number of rows and columns in the text file header) are parsed and used to dimension the two-dimensional array.

In the case of modelling natural processes with complex dynamics such as fire propagation, several factors such as topography, vegetation, etc. are important and their values need to be accessed in each cell in order to be able to implement some of the complex mathematical models. This constitutes a relaxation of traditional CA rules where sole reliance on the state of neighbouring cells (e.g. burning) and a measure of suitability for the particular cell is not adequate.

Given that any raster image can be stored in a two-dimensional array, the GIS raster layers of all the factors involved in the environmental model can be stored in two-dimensional arrays which in turn will provide access to the values of these factors for each individual cell. All the GIS raster layers used in the model are geo-referenced to the same geographical area and have the same resolution and dimensions. For example, elevation, slope, and fuel type raster layers can be stored in arrays *elevArray*, *slopeArray*, and *fuelArray*; this provides access to the slope, aspect and fuel type values of each cell in the CA grid. Specifically the values of elevation, slope and fuel type of (i, j) cell will be *elevArray* (i, j), *slopeArray* (i, j), *fuelArray* (i, j) and so on as presented in Fig. 8.

The programming language provides considerable flexibility in choosing the neighbours of each cell (e.g. type and size) and implementing complex transition rules. The result after the desired number of time steps (iterations) is written to a text file from the fire array (programmatically) and converted to a raster image (by calling Idrisi's conversion function) to be visualized in GIS. During the simulation, this method creates a final output of stacked raster layers in the GIS where each layer represents the spatial change after the desired time interval.

The method of stacking raster layers is a standard way of visualizing dynamic processes in GIS. An improvement to such visualization is made by initially specifying and displaying a base layer (e.g. fuel type, DEM, aspect, etc.); and at the end of each desired time interval the output (fire) raster layer is converted to a vector layer which is added to the base raster map (automated as above by calling Idrisi's functions). Consecutive addition of vector layers after each time interval to the same base map results in a dynamic animated simulation. Fig. 9 presents a flow diagram of the steps involved in the GIS-CA model integration.

4.1. *Development of the user interface*

An intuitive, flexible, and user-friendly interface was developed to make the model accessible to a wider audience who might not have GIS expertise (e.g. fire managers, researchers).

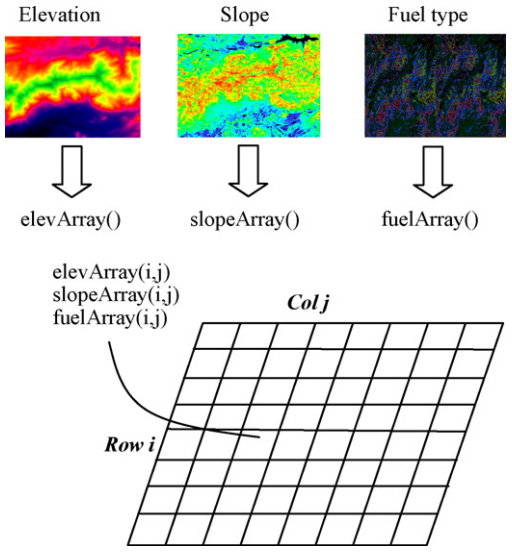

Fig. 8 – Accessing values of individual cell characteristics.

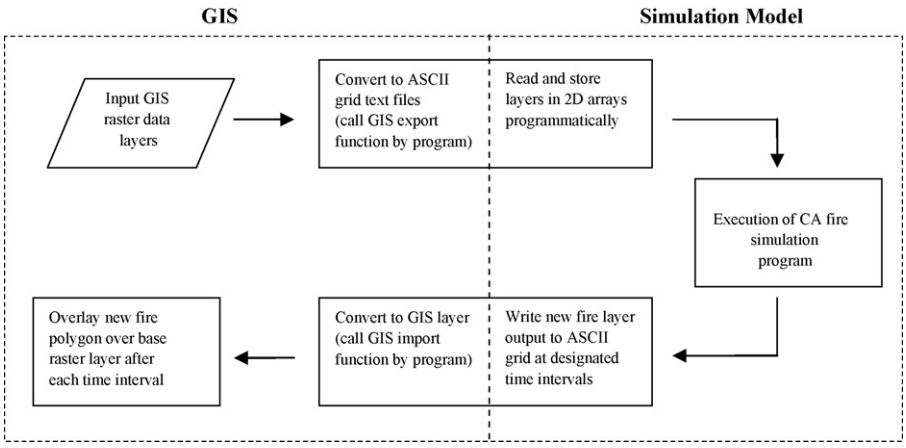

Fig. 9 – Flow diagram of GIS–CA model integration: all input and output data are stored in a working folder; simulation is automated by making function calls to GIS and by programmatically reading and writing ASCII grid files.

This allows the end-user to take advantage of the essential GIS and modelling functionality without the need for interaction with the software tools. The user interface for the fire behaviour model is categorized into logical sections to provide the user with options for data input, simulation timing and visualization. The user form can be positioned at any location on the Idrisi interface as shown in Fig. 10. This allows simultaneous interaction with the interface and the outcome results generated.

4.1.1. *Data input*

The model inputs are selected by the user from the drop-down combo boxes. These inputs are raster layers (or corresponding ASCII text files) of fuel type, slope, aspect, and the fire ignition (starting position of fire which can be point, line or polygon).

4.1.2. *Simulation timing*

The weather text file (data stream) is also selected by the user together with the simulation start and stopping time. The

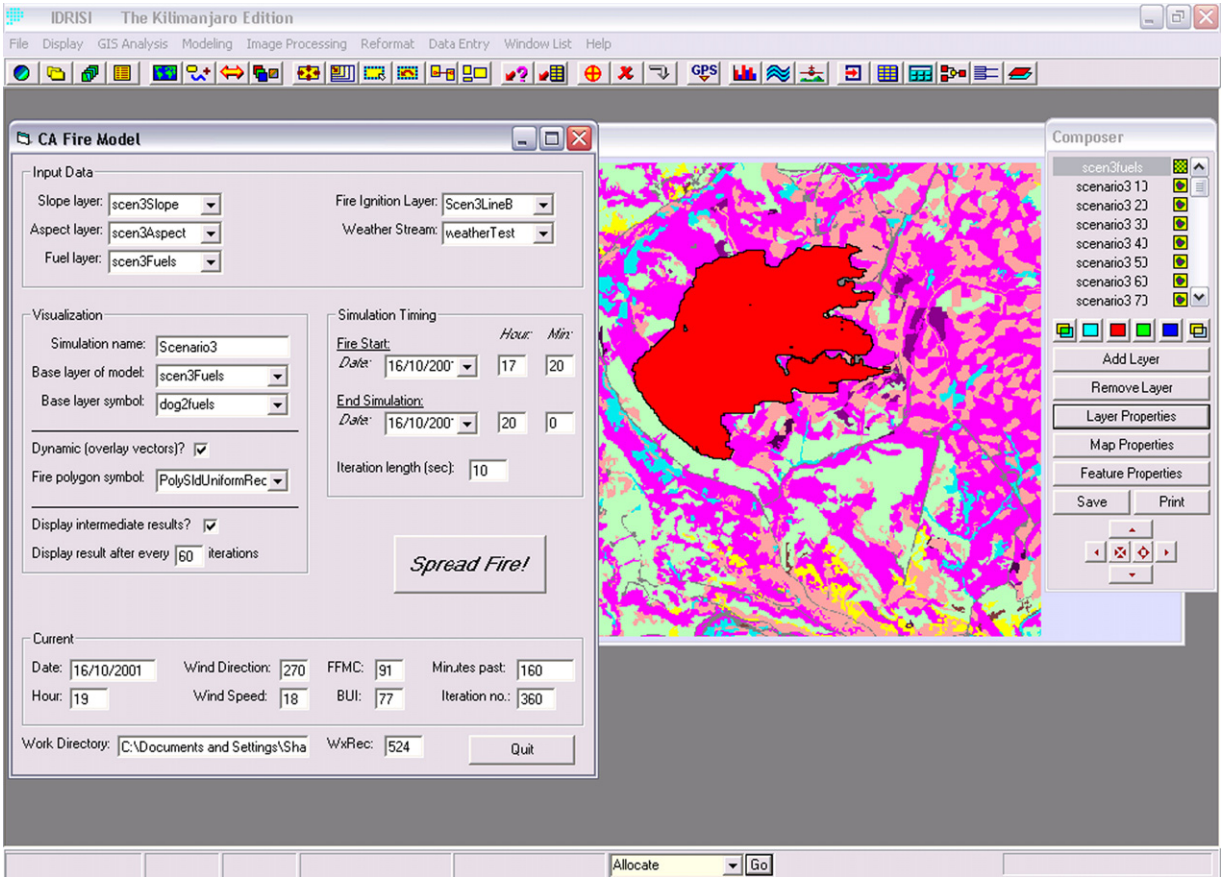

Fig. 10 – Fire behaviour model user interface.

program accesses the weather records corresponding to the chosen period and incorporates the current hourly values for the weather factors (e.g. wind speed and direction). As the simulation progresses, the corresponding values for each hour are used. The desired iteration length (time step) is selected by the user. The iteration length should be selected such that during each time step the distance of fire travel does not extend beyond one cell length. The case of expanded neighbourhoods is not considered in this study as the fire spread across more than one cell in a time step can propagate aggregation errors into the model outcome. In general a smaller time step would provide more realistic results.

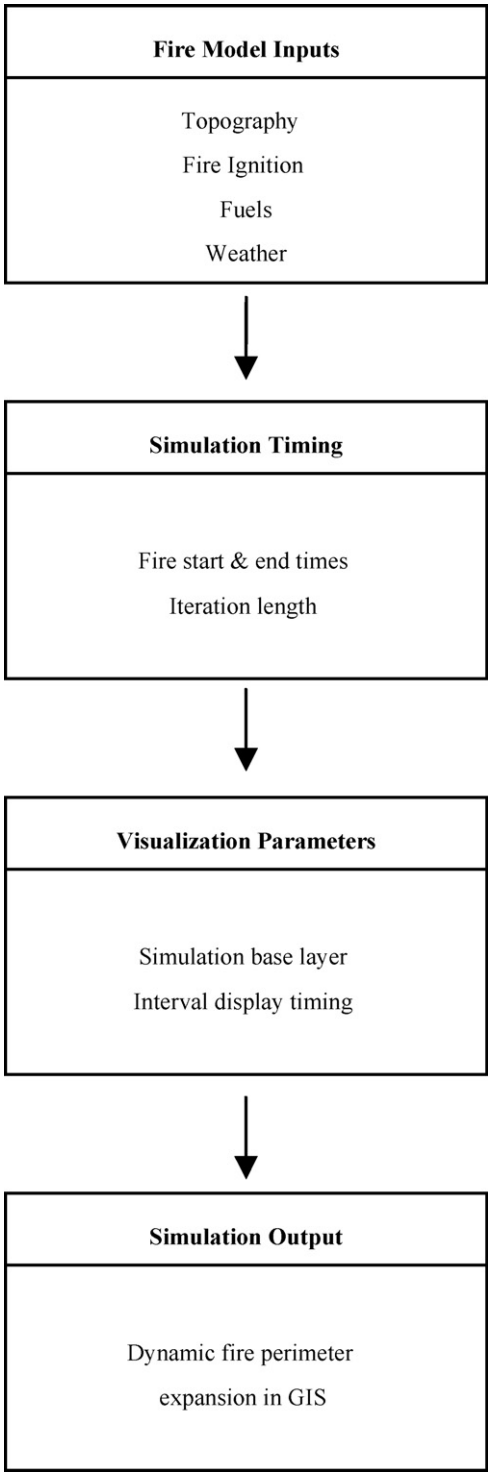

Fig. 11 – Steps involved in running the modeling tool.

4.1.3. *Visualization*

The user has the option to view the dynamic simulation of fire spread on top of a desired base raster layer (e.g. fuel type, DEM, aspect, etc.). An Idrisi symbol file can be used to render the chosen base layer. There is an option to choose dynamic animation on top of the base layer or to stack the raster layers. The fire layer can be rendered with various symbols such as solid polygon or enclosed polyline. Also, the user has the option of displaying the intermediate results after a specified number of iterations or just displaying the final simulation result. For example with a 10 s time step, displaying intermediate results after 60 iterations indicates an interval of 10 min. The simulation results are displayed on the Idrisi interface. The user can use the 3D functionality of Idrisi to drape each resultant layer on the 3D landscape (can be automated) or use the 3D fly through module to interact with the landscape and observe the simulation results from different directions and angles. Further, the map composer of Idrisi can be used to hide/remove any interval result or explore each interval result individually. The burned polygon area and perimeter at the end of a specified time interval are saved as a text file.

4.1.3.1. Current conditions. At the bottom of the form the current conditions including the time, wind speed and direction, temperature, etc. are updated after each interval. Other variables of interest to the user for observation during the simulation can be added to the display set. Fig. 11 summarises the steps taken in running the modeling tool.

5. Results

The test dataset used was from the Dogrib Fire near Nordegg, Alberta, Canada which started on 25 September 2001. This is the example dataset documented in the Prometheus manual (Prometheus User Manual, 2004) and was used in this study as it contains detailed fuel, weather and fire perimeter information for this fire. The raster data has a cell resolution of 25 m. There were a variety of fuel types at the site including Boreal Spruce, Jack Pine/Lodgepole Pine, grass, and Aspen among others. The fire burned for 22 days. During this time, the fire weather (FWI) indices were high and fuel moisture conditions were very dry. For the first 21 days, there were normal spread conditions with respect to the FWI indices and the fire reached a size of 828 ha on the evening of October 15th, 2001. On October 16th a major wind event occurred with wind gusts of over 100 km/h. The fire burned 92% of the final size in the afternoon period, reaching a size of 9898 ha. The fire traveled a distance of 24.6 km during this period which equates to an average rate of spread of 30 m/min (Prometheus User Manual, 2004).

The Dogrib Fire was driven by both wind and convection. The prevailing winds were from the southwest. The varying topography created complex wind effects. Long-range spotting also occurred where head of fire skipped from the top of one ridge to the next leaving unburned fuel in between. Mod-

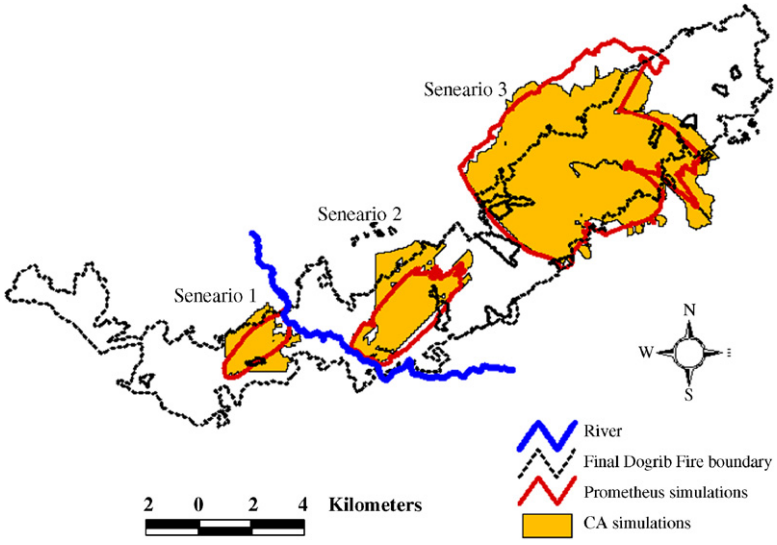

Fig. 12 – Prometheus and CA simulations and final actual fire boundary.

elling such a complex fire is very difficult (Prometheus User Manual, 2004) and hence three different scenarios were considered in Prometheus, each with a separate initial ignition. Simulations performed in Prometheus provide a reasonable growth projection. However, since wind gusts were not incorporated, the projection underestimated the final length (size) of the fire (Prometheus User Manual, 2004). To account for some of the topographic effects on wind, wind speed and wind direction grids can be used with Prometheus. These grids can be incorporated into the CA model as well by treating the wind grid in a similar way as the other raster layers.

The three scenarios used in Prometheus were replicated with the CA fire model using the same input data (i.e. fuel, topography, weather). Fig. 12 shows the overview map of the study area indicating the location of the three scenarios along with the boundary of the actual burned area after the fire event. Fig. 13(a–l) presents the simulation results for the three scenarios with four different time intervals for each scenario. Solid polygons represent fire perimeters for the CA model and enclosed lines represent fire boundaries generated by Prometheus simulations.

5.1. *Scenario 1*

A point source ignition is used in this scenario which was assumed to be the actual fire location on 16 October 2001 just before the major fire spread event started (i.e. assumption is that the fire polygon from previous days had already mostly burnt out by this time). The simulation ran from 13:00 to 15:40 hours at which point the fire reached the Red Deer River. Wind gusts between 100 and 130 km/h were reported some time after 13:00 hours.

The difference in the extent of burned area between Prometheus and CA model simulations in this scenario may be attributed to the fact that Prometheus accounts for acceleration of fire when using point source ignitions. Therefore, it takes the fire longer to reach an equilibrium rate of spread when the fire starts from the point source ignition using the Prometheus simulation. On the other hand, the CA model at this time assumes equilibrium fire spread rate for all ignition sources (i.e. point, line, and polygon).

5.2. *Scenario 2*

Although southwest winds were prevalent during this fire event, the funnelling of the wind along the Red Deer River and through a gap in the mountains pulled the fire slightly towards the southeast. A new line source of ignition is used to represent the fire spotting across the river. Spotting distances of up to 2 km were observed. This simulation ran from 15:40 to 17:20 hours.

5.3. *Scenario 3*

This scenario represents the start of spot fires across the second ridge with a new line source ignition at 1720 hours. The simulation was run until 22:00 hours for a total time of 4 h 40 min. At this time the fire stopped spreading.

6. Model evaluation

The visual inspection of the generated simulation maps indicate a good agreement between the CA model and Canadian fire growth model (Prometheus, based on the more computationally intensive elliptical wave propagation principle) in complex heterogeneous conditions. The CA results indicated that it is more sensitive to variations in conditions (e.g. fuel, slope, aspect) at the cell level and can assume more irregular shapes in response to these variations as opposed to the wave model's more compact elliptical shapes.

Following the above observation, a test was conducted to confirm the relative sensitivity of the two modeling approaches at the cell level. Fig. 14 compares the response of the two models to changes in topography under homogeneous fuel and zero wind conditions. Simulations were done for a line ignition source situated along a valley bottom with higher

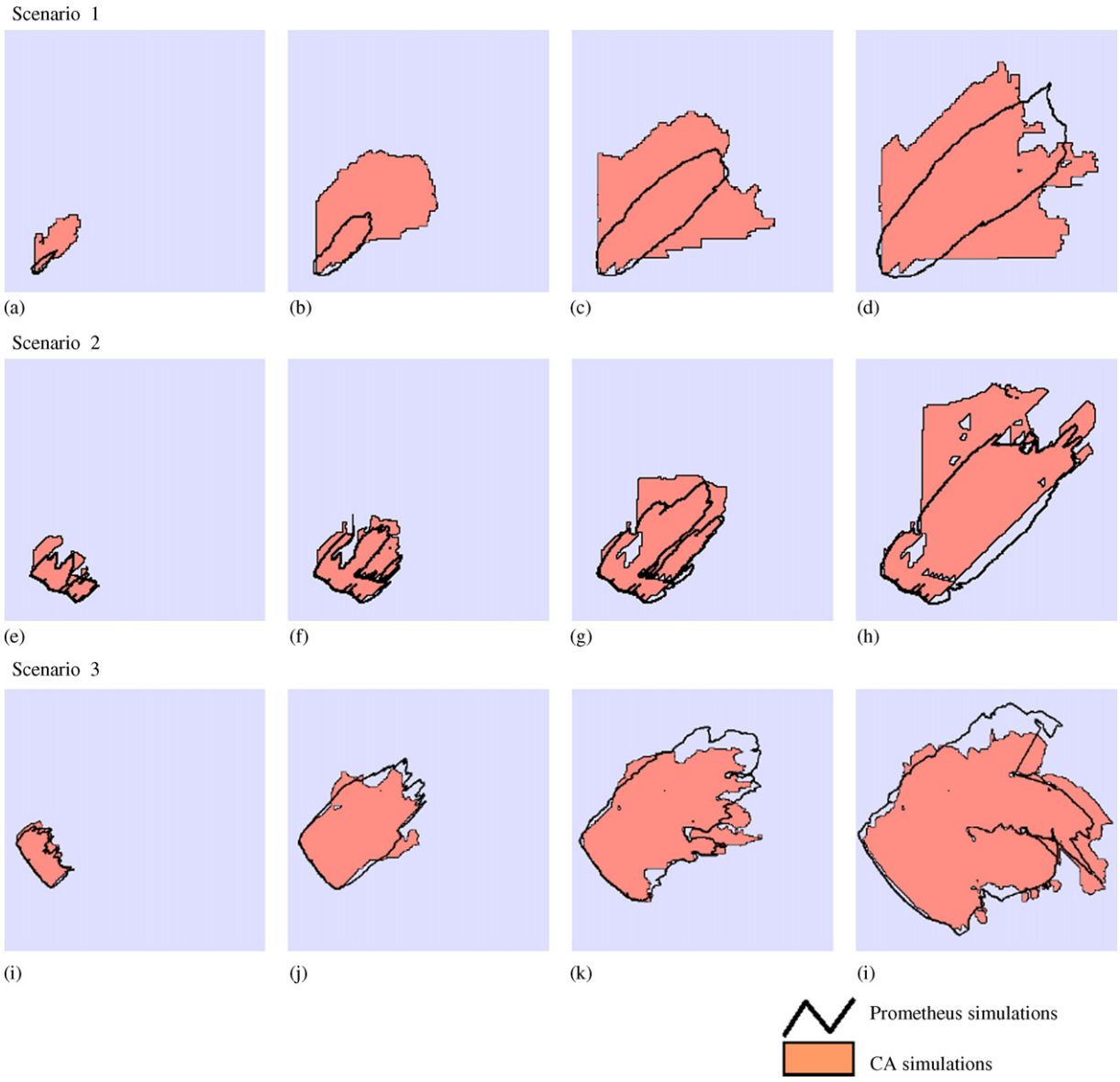

Fig. 13 – Dogrib fire simulations comparing CA model vs. Prometheus, Scenario 1: (a) 40 min; (b) 80 min; (c) 120 min; (d) 160 min, Scenario 2: (e) 20 min; (f) 40 min; (g) 60 min; (h) 100 min, Scenario 3: (i) 20 min; (j) 80 min; (k) 160 min; (l) 280 min.

grounds to the left and right (steeper slope and highest point to the right). Solid polygons represent fire perimeters for the CA model and enclosed polylines represent the Prometheus simulations. The CA simulations are more sensitive to slight changes in topography where the fire moves towards steeper contours and consequently the fire assumes a more irregular shape (as seen rushing up the steepest part of the hill to the right). The Prometheus simulations show more regular growth shapes without acute response to changes in topography. In the CA model, the fire spread on flat ground (i.e. low WSV) is less in comparison to Prometheus.

The CA model with current transition rules responds well to the conditions of high *net wind* (WSV) conditions (where head fire spread is the main driving force of the fire) as well as heterogeneous fuel types. However, the CA model's performance decreases in more homogeneous fuel conditions and lower WSV (i.e. gentle slope and/or gentle wind) where the back and flank rates assume more importance and the length to breath ratio of the elliptical fire decreases. In order to address the low WSV conditions the transition rules are relaxed, and for WSV zero condition (flat ground and single fuel type), the angles are set so that fire travels in the most direct direction in all eight neighbouring cells. Further, in a homogeneuos fuel condition and flat ground with the wind blowing from one of the four cardinal directions perpendicular to a line of fire, the CA simulation of a line fire would result in a rectangular shape, while more diagonal wind directions would result in a parallelogram. These shapes do not correlate fully with the general ellipsoidal shapes that are characteristic of homogeneous conditions.

The case of homogeneous conditions with gentle wind speed can be addressed by developing a sub-model for these conditions and integrating it with the present model. In addition, an established model such as Anderson's (2002)

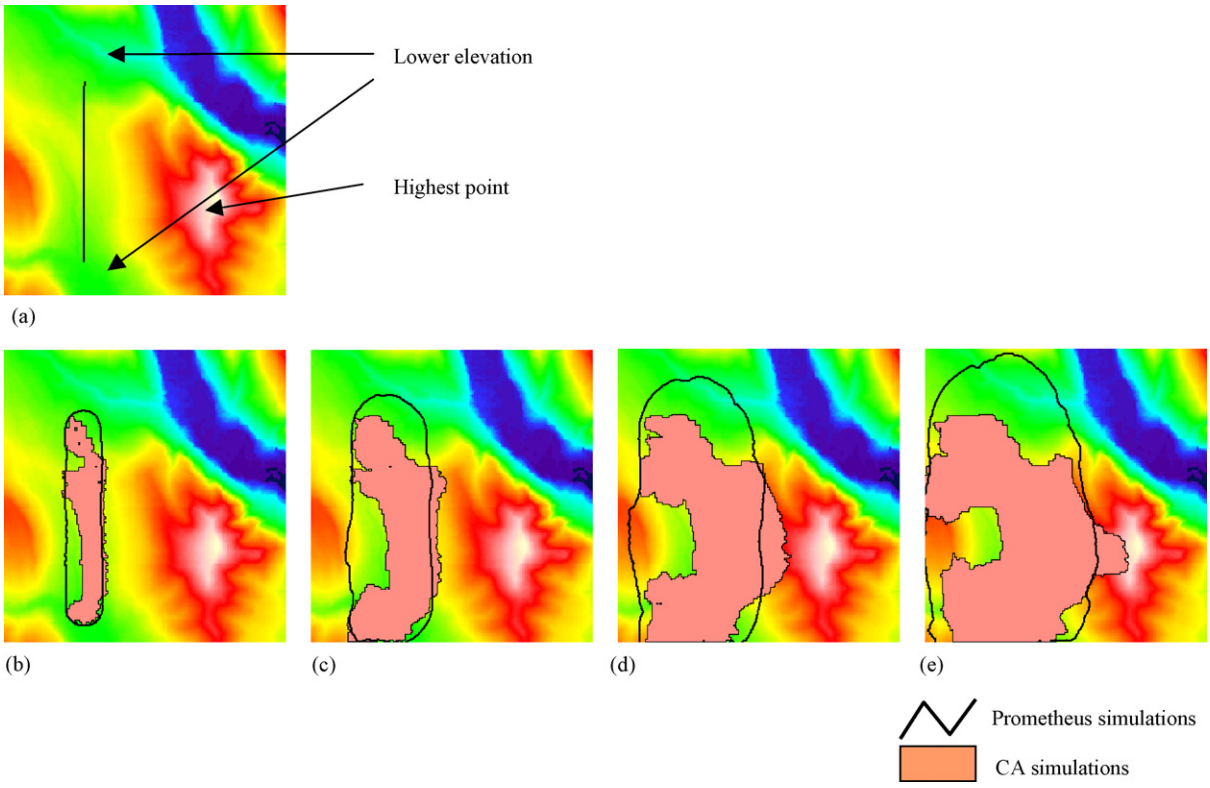

Fig. 14 – Comparison of CA model vs. Prometheus simulations with changes in topography under homogeneous fuel and zero wind conditions: (a) initial ignition line; (b) 60 min; (c) 120 min; (d) 180 min; (e) 240 min.

short-range cellular model or the elliptical wave model can be integrated and used to model fire spread under these conditions.

7. Discussion and conclusion

This study confirms the potential of the CA approach for fire behaviour modelling; more systematic tests utilizing all the FBP fuel models under a variety of weather and topographic conditions need to be conducted. Moreover comparisons with a variety of real fire events are required before a definitive statement on the validity of the CA model can be made.

The empirical nature of the FBP model served as the basis of the CA model limits the applicability of the model to regions with the specific FBP or similar fuel types. However, the present CA model can be regarded as a generic simulation technique that can be based on other physical, empirical or semi-empirical models. This in turn would enable further exploration of the model in other ecosystems and evaluation of this CA approach against other established wave propagation or CA models. For example a comparison with the *FARSITE* (Finney, 2004) wave model can be accomplished by the use of Rothermel's (1972) semi-empirical model and other sub-models that form the basis of *FARSITE*'s simulation technique. Similarly the performance of the CA model against the Australian *SiroFire* (Coleman and Sullivan, 1996) wave model can be evaluated by employing McArthur's (Noble et al., 1980) empirical model which forms the basis of *SiroFire*.

By providing an effective way for integration of CA-based modelling with GIS, the approach developed in this study can be adopted for use in other CA-based environmental modelling applications. The GIS software allows the use of any COM-compliant programming language. The modeling tool can be added as a customized module within Idrisi GIS. Furthermore, the interface can be designed to provide the general user with automated access to extensive GIS functionalities of Idrisi; and a variety of tools in support of modelling activities such as spatial analysis, remote sensing image analysis, spatial data management, decision support, and visualization among others can be made accessible to the user within the same environment.

Direct comparisons of the validity of different simulation techniques can be drawn only on the basis of the same fuel and fire characteristics models and based on applications to real fire events. Therefore, it is not a trivial task to compare the superiority of one simulation technique against another where they utilize different fuel and fire characteristics models or employ different types of transition rules (e.g. deterministic versus stochastic). However, some general observations of CA simulation techniques can be made based on comparison of such transition rules.

The developed CA model in this study employs a deterministic simulation technique similar to those of Karafyllidis and Thanailakis (1997) and Berjak and Hearne (2002). Berjak and Hearne improved on Karafyllidis and Thanailakis's model; therefore some specific improvements over Berjak and Hearne's model are presented below. Further, general advan-

tages of the new CA model not considered in other CA fire studies are noted.

Berjak and Hearne, similar to this study, calculate the fraction of the cell burned after a discrete time interval. In their study, empirical slope, wind and fuel heterogeneity factors appropriate for the local conditions were incorporated in order to modify the rate of fire spread attained by Rothermel's (1972) model for homogeneous, flat and windless conditions. However, in their model the effect of slope direction (i.e. aspect) is not taken into account, and furthermore the combined effect of aspect and wind direction providing the fire spread direction within each cell is not considered. Such omission would prevent the use of vector components as employed in this study. Whereas in this study the net wind direction (aspect and wind) can be anywhere between 0 and 360 degrees, in Berjak and Hearn's model wind direction is only restricted to the eight major compass directions. Again such restriction prevents finer calculations of fire spread direction within and between cells.

In general two techniques have been employed in this study, which are not observed in Berjak and Hearne's as well as other CA models. First, a limiting fire direction range for the burning neighbouring cells was applied as a pre-condition of fire spread to the central cell. This technique was successful in synchronization of the spread of fire with the net wind direction. Second, the overlap of burning areas within a cell as the result of fire spread contribution from multiple neighbours is accounted for. Both techniques were found to be very effective in preventing overestimation of fire spread area.

As evident from existing fire simulation models, deterministic models that take into account complex interactions of fuel type and moisture, topography and weather factors, are effective in modeling short term fire behaviour. Short term fire modeling is based on the assumption that the input meteorological data are accurate and reliable (Anderson, 2002). However, due to the inability to accurately predict weather conditions beyond few days (Smagorinsky, 1967), deterministic rules will not be adequate in calculating medium to long-range fire behaviour. Therefore, with the broadening of scale in space and time, and consequent lack of detailed input data, some studies suggest incorporation of probabilistic, stochastic, or self-organized criticality rules (Ito, 2005; Anderson, 2002; Song et al., 2001).

Similarly some wildland fire characteristics such as spotting may not be adequately explained by deterministic rules. Therefore, a combination of deterministic and stochastic (Clarke et al., 1994) rules may be used to develop a more comprehensive model. For example, during extreme fire events involving torching of trees and crown fires, the existing deterministic spread between cells can be augmented by introducing stochastic rules for the travel of fire brands, where cells downwind of the current fire perimeter can act as new points of ignition during the next time step.

Finally it should be noted that it is imperative for simulation models to have a validated fire behavior model incorporating weather, topography, and vegetation as their basis in order to provide the essential fire characteristic inputs needed for simulation. Simulations with good results in hypothetical conditions (Encinas et al., 2007; Cormas, 2007; Li and Magill, 2001; Karafyllidis and Thanailakis, 1997) without using such empirical, semi-empirical or physical models may not produce realistic results when applied to real fire events.

Acknowledgements

This study is supported by the Natural Sciences and Engineering Research Council (NSERC) of Canada under a Discovery Grant Programs awarded to second and third authors. We gratefully acknowledge the assistance of Mike Wotton and Kerry Anderson of the Canadian Forest Service for providing relevant reference materials and information regarding the Canadian Fire Behaviour Prediction System. In addition, we thank the anonymous reviewers and journal editor for their constructive and valuable comments.

REFERENCES

Albright, D., Meisner, B.N., 1999. Classification of fire simulation systems. USDA For. Serv. Fire Mgt. Notes 59, 5–12.

Anderson, D.H., Catchpole, E.A., DeMestre, N.J., Parkes, T., 1982. Modelling the Spread of grass fires. J. Aust. Math. Soc. B 23, 451–466.

Anderson, K.R., 2002. Fire growth modelling at multiple scales. In: Viegas, D.X. (Ed.), Proceedings of the IVth International Conference on Forest Fire Research and Wildland Fire Safety. Luso-Coimbra, Portugal. Millpress Sci. Publ, Rotterdam, Netherlands, p. 6.

Andrews, P.L., 1986. BEHAVE: fire behavior prediction and fuel modeling system-BURN subsystem, Part 1. USDA For. Serv., Intermt. For. Range Exp. Stn. Ogden, UT. Gen. Tech. Rep. INT-194, 130 pp.

Andrews, P.L., Queen, L.P., 2001. Fire modeling and information system technology. Int. J. Wildland Fire 10, 343–352.

Balzter, H., Braun, P.W., Kohler, W., 1998. Cellular automata models for vegetation dynamics. Ecol. Model. 107, 113–125.

Batty, M., Xie, Y., 1994. From cells to cities. Environ. Plann. B Plann. Des. 21, S31–S38.

Beer, T., Enting, I.G., 1990. Fire Spread and Percolation Modeling. Math. Comput. Model. 13, 77–96.

Berjak, S.G., Hearne, J.W., 2002. An improved cellular automaton model for simulating fire in a spatially heterogeneous Savanna system. Ecol. Model. 148, 133–151.

Bone, C., Dragicevic, S., Roberts, A., 2006. A fuzzy-constrained cellular automata model of forest insect infestations. Ecol. Model. 192, 107–125.

Burrough, P.A., McDonnell, R.A., 1998. Principles of geographical information systems. Oxford University Press, Oxford, 356 pp.

Cannas, S.A., Marco, D.E., Paez, S.A., 2003. Modelling biological invasions: species traits, species interactions, and habitat heterogeneity. Math. Biosci. 183, 93–110.

Clark Labs, Last accessed in Nov. 2005 from, http://www.clarklabs.org/, 2004.

Clarke, K.C., Brass, J.A., Riggan, P.J., 1994. A Cellular-Automaton Model of Wildfire Propagation and Extinction. Photogramm. Eng. Rem. S. 60, 1355–1367.

Clarke, K.C., Gaydos, L.J., 1998. Loose-coupling a cellular automaton model and GIS: long-term urban growth prediction for San Francisco and Washington/Baltimore. Int. J. Geogr. Inf. Sci. 12, 699–714.

Clarke, K.C., Parks, B.O., Crane, M.P. (Eds.), 2002. Geographic Information Systems and Environmental Modeling. Prentice Hall, New Jersey, 306 pp.

Coleman, J.R., Sullivan, A.L., 1996. A real-time computer application for the prediction of fire spread across the Australian landscape. Simulation 67 (4), 230–240.
Cormas 2007. Cormas Natural Resources and Multi-Agent Simulations Software. Fire Agent Model. Last accessed in June 2007 from: http://cormas.cirad.fr/en/outil/classroom/example/FireModel/index.htm.
Darwen, P.J., Green, D.G., 1996. Viability of populations in a landscape. Ecol. Model. 85, 165–171.
De Vasconcelos, M.J.P., Goncalves, A., Catry, F.X., Paul, J.U., Barros, F., 2002. A working prototype of a dynamic geographical information system. Int. J. Geogr. Inf. Sci. 16, 69–91.
Dragicevic, S., Marceau, D.J., 2000. A fuzzy set approach for modeling time in GIS. Int. J. Geogr. Inf. Sci. 14, 225–245.
Encinas, A.H., Encinas, L.H., White, S.H., del Rey, A.M., Sanchez, G.R., 2007. Simulation of forest fire fronts using cellular automata. Adv. Eng. Soft. 38, 372–378.
Finney, M.A., 2004. FARSITE: Fire Area Simulator–Model Development and Evaluation. Rocky Mtn. Res. Stn., USDA. Res. Paper RMRS-RP-4 Revised, 47 pp.
Forestry Canada Fire Danger Group, 1992. Development and structure of the Canadian forest fire behaviour prediction system. Forestry Canada, Ottawa, ON. Inf. Rep. ST-X-3, 63 pp.
French, I.A., 1992. Visualisation techniques for the computer simulation of bushfires in two-dimensions. M.S. Thesis, University of New South Wales, 140 pp.
Grist, E.P.M., 1999. The significance of spatio-temporal neighbourhood on plant competition for light and space. Ecol. Model. 121, 63–78.
Hargrove, W.W., Gardner, R.H., Turner, M.G., Romme, W.H., Despain, D.G., 2000. Simulating fire patterns in heterogeneous landscapes. Ecol. Model. 135, 243–263.
Hirsch, K.G., 1996. Canadian forest fire behaviour prediction (FBP) system: user's guide. Canadian Forest Service, Northern Forestry Centre. Spec. Rep. 7, 122 pp.
Ito, A., 2005. Modelling of carbon cycle and fire regime in an east Siberian larch forest. Ecol. Model. 187, 121–139.
Johnson, E.A., Miyanishi, K. (Eds.), 2001. Forest Fires: Behavior and Ecological Effects. Academic Press, San Diego, 600 pp.
Jordan, G.J., Fortin, M.J., Lertzman, K.P., 2005. Assessing spatial uncertainty associated with forest fire boundary delineation. Landscape Ecol. 20, 719–731.
Karafyllidis, I., Thanailakis, A., 1997. A model for predicting forest fire spreading using cellular automata. Ecol. Model. 99, 87–97.
Kourtz, P.H., O'Regan, W.G., 1971. Model for a small forest fire to simulate burned and burning areas for use in a detection model. Forest Sci. 17, 163–169.
Kourtz, P., Nozaki, S., O'Regan, W., 1977. Forest fires in the computer–A model to predict the perimeter location of a forest fire. Fisheries and Environment Canada. Inf. Rep. FF-X-65.
Lee, B.S., Alexander, M.E., Hawkes, B.C., Lynham, T.J., Stocks, B.J., Englefield, P., 2002. Information systems in support of wildland fire management decision making in Canada. Comput. Electron. Agr. 37, 185–198.
Li, X., Magill, W., 2001. Modeling fire spread under environmental influence using a cellular automaton approach. Complexity Intl., 8: Paper ID: li01. Last accessed in June 2007 from: http://www.complexity.org.au/ci/vol08/li01/.
Matsinos, Y.G., Troumbis, A.Y., 2002. Modeling competition, dispersal and effects of disturbance in the dynamics of a grassland community using a cellular automaton model. Ecol. Model. 149, 71–83.
Mitasova, H., Mitas, L., 2002. Modeling physical systems. In: Clarke, K.C., Parks, B.O., Crane, M.P. (Eds.), Geographic Information Systems and Environmental Modeling. Prentice Hall, New Jersey, pp. 189–210.
Morley, P.D., Chang, J., 2004. Critical behavior in cellular automata animal disease transmission model. Int. J. Mod. Phys. C 15, 149–162.
Noble, I.R., Barry, G.A.V., Gill, A.M., 1980. McArthur's fire-danger meter expressed as equations. Aust. J. Ecol. 5, 201–203.
Pastor, E., Zarate, L., Planas, E., Arnaldos, J., 2003. Mathematical models and calculation systems for the study of wildland fire behaviour. Prog. Energ. Combust. 29, 139–153.
Prometheus, 2004. The Canadian Wildland Fire Growth Model (CWFGM), Prometheus ver. 3.2.3. Last accessed in Nov. 2005 from http://www.firegrowthmodel.com/index.cfm.
Prometheus User Manual, Last accessed in Nov. 2005 from, http://www.firegrowthmodel.com/public_download.cfm, 2004.
Richards, G.D., 1988. Numerical-simulation of forest fires. Int. J. Numer. Methods. Eng. 25, 625–633.
Richards, G.D., 1995. A general mathematical framework for modeling 2-dimensional wildland fire spread. Int. J. Wildland Fire 5, 63–72.
Rothermel, R.C., 1972. A mathematical model for predicting fire spread in wildland fuels. USDA For. Serv., Ogden, UT. Res. Paper INT-115, 40 pp.
Rothermel, R.C., 1983. How to predict the spread and intensity of forest and range fires. USDA For. Serv. Intermt. For. Range Exp. Stn., Ogden, UT. Gen. Tech. Rep. INT-143, 53 pp.
Sirakoulis, G.C., Karafyllidis, I., Thanailakis, A., 2000. A cellular automaton model for the effects of population movement and vaccination on epidemic propagation. Ecol. Model. 133, 209–223.
Smagorinsky, J., 1967. The role of numerical modeling. Bull. Am. Meteoro. Soc. 48 (2), 89–93.
Smyth, C.S., 1998. A representational framework for geographic modeling. In: Egenhofer, M.J., Golledge, R.G. (Eds.), Spatial and Temporal Reasoning in Geographic Information Systems. Oxford University Press, New York, pp. 191–213.
Song, W., Weicheng, F., Binghong, W., Jianjun, Z., 2001. Self-organized criticality of forest fire in China. Ecol. Model. 145 (1), 61–68.
Van Wagner, C.E., 1969. A simple fire-growth model. Forest Chron. 45, 103–104.
Van Wagner, C.E., 1987. Development and structure of the Canadian Forest Fire Weather Index System. Canadian Forest Service, Ottawa. ON. For. Tech. Rep. 35, 37 pp.
Von Neumann, J., 1966. The Theory of Self-reproducing Automata. University of Illinois Press, Urbana, IL, 388 pp.
Waters, N., 2002. Modeling the environment with GIS: a historical perspective from geography. In: Clarke, K.C., Parks, B.O., Crane, M.P. (Eds.), Geographic Information Systems and Environmental Modeling. Prentice Hall, New Jersey, pp. 1–35.
White, R., Engelen, G., 1997. Cellular automata as the basis of integrated dynamic regional modelling. Environ. Plann. B – Plann. Des. 24, 235–246.
White, R., Engelen, G., 2000. High-resolution integrated modeling of the spatial dynamics of urban and regional systems. Comput. Environ. Urban 24, 383–400.
Wu, F.L., Webster, C.J., 2000. Simulating artificial cities in a GIS environment: urban growth under alternative regulation regimes. Int. J. Geogr. Inf. Sci. 14, 625–648.
Yang, L.Z., Fang, W.F., Huang, R., Deng, Z.H., 2002. Occupant evacuation model based on cellular automata in fire. Chinese Sci. Bull. 47, 1484–1488.
Ziegler, B.P., 1990. Object Oriented Simulation With Hierarchical Modular Models: Intelligent Agents and Endomorphic Systems. Academic Press, 395 pp.